HHS Public Access

Author manuscript

J Bone Miner Res. Author manuscript; available in PMC 2018 September 01.

Published in final edited form as:

J Bone Miner Res. 2017 September ; 32(9): 1884–1892. doi:10.1002/jbmr.3180.

Hypermineralization and high osteocyte lacunar density in osteogenesis imperfecta type V bone indicate exuberant primary bone formation

Stéphane Blouin, PhD[1], **Nadja Fratzl-Zelman, PhD**[1], **Francis H Glorieux, MD, PhD**[3], **Paul Roschger, PhD**[1], **Klaus Klaushofer, MD, PhD**[1], **Joan C. Marini, MD, PhD**[2], and **Frank Rauch, MD, PhD**[3]

[1]Ludwig Boltzmann Institute of Osteology at the Hanusch Hospital of WGKK and AUVA Trauma Centre Meidling, 1st Medical Department Hanusch Hospital, Vienna, Austria

[2]Bone and Extracellular Matrix Branch, NICHD, NIH, Bethesda, MD, USA

[3]Shriners Hospital for Children, Montreal, Quebec, Canada

Abstract

In contrast to “classical” forms of Osteogenesis imperfecta (OI) types I to IV, caused by a mutation in *COL1A1/A2*, OI type V is due to a gain-of-function mutation in the *IFITM5* gene, encoding the interferon-induced transmembrane protein 5, or bone-restricted ifitm-like protein (BRIL). Its phenotype distinctly differs from OI types I to IV by absence of blue sclerae and dentinogenesis imperfecta, by the occurrence of ossification disorders like hyperplastic callus and forearm interosseous membrane ossification. Little is known about the impact of the mutation on bone tissue/material level in untreated and bisphosphonate treated patients.

Therefore investigations of transiliac bone biopsy samples from a cohort of OI type V children (n=15, 8.7±4 years old) untreated at baseline and a subset (n=8) after pamidronate treatment (2.6 years in average) were performed. Quantitative backscattered electron imaging (qBEI) was used to determine bone mineralization density distribution (BMDD) as well as osteocyte lacunar density. The BMDD of type V OI bone was distinctly shifted towards higher degree of mineralization. The most frequently occurring calcium concentration (CaPeak) in cortical (Ct) and cancellous (Cn) bone was markedly increased (+11.5%, +10.4%, respectively, P<0.0001) compared to healthy reference values. Treatment with pamidronate resulted in only a slight enhancement of mineralization. The osteocyte lacunar density derived from sectioned bone area was elevated in OI type V Ct and Cn bone (+171%, P<0.0001 and +183.3%, P<0.01, respectively) versus controls. The high osteocyte density was associated with an overall immature primary bone structure (”mesh-like”) as visualized by polarized light microscopy.

In summary the bone material from OI type V patients is hypermineralized, similarly to other forms of OI. The elevated osteocyte lacunar density in connection with lack of regular bone

Corresponding author: Dr. Stéphane BLOUIN, Ludwig Boltzmann Institute of Osteology, UKH Meidling, Kundratstr. 37, A-1120 Vienna, Austria; stephane.blouin@osteologie.at, Phone number: +43 5 93 93 55 769.

DISCLOSURES

All authors state that they have no conflicts of interest

lamellation points to an exuberant primary bone formation and an alteration of the bone remodeling process in OI type V.

Keywords

Osteogenesis imperfecta type V; quantitative Backscattered Electron Imaging; Matrix mineralization; Osteocyte lacunae; Bisphosphonate treatment

INTRODUCTION

Osteogenesis imperfecta (OI) is a heritable connective tissue disorder whose primary features are bone fragility, frequently resulting in bone deformities, and growth deficiency [1,2]. The “classical” OI types I to IV are caused by autosomal dominant inheritance of mutations in *COL1A1* or *COL1A2*, the genes encoding type I procollagen α-chains, and differing mainly by the severity of their clinical phenotype [2]. During the last decade, a large number of defects in non-collagenous genes have been associated with mostly autosomal recessive forms of OI [3].

OI type V was the first type of OI in which no mutation in a collagen type I encoding gene could be found [4]. The most conspicuous clinical characteristics of OI type V are the susceptibility to hyperplastic callus formation after fracture or surgery, new bone formation along the interosseous membrane of the forearm, leading to radial head dislocation, and a subphyseal radiodense line [4,5]. Blue sclera and dentinogenesis imperfecta, typical features in OI types I to IV, are absent in OI type V. On the level of bone histology, the most consistent feature of OI type V is an altered lamellation pattern that results in a ”mesh-like” appearance of the bone tissue under polarized light [4–7]. A broad range of disease severity has been observed in the approximately 100 individuals with OI type V who have been reported in the literature [5,8–13]. Iliac bone histomorphometry in OI type V has revealed low trabecular bone volume and a low bone formation rate, which is in contrast to OI caused by collagen type I mutations, where bone formation rate is typically elevated [4,14].

In 2012 two groups independently identified a *de novo* heterozygous mutation in *IFITM5,* the gene encoding the interferon-induced transmembrane protein 5, also called bone-restricted ifitm-like protein (BRIL) [9,11]. BRIL is expressed in osteoblasts and may play a role in early mineralization stages [15,16]. A recurrent point mutation (*IFITM5* c.–14C>T) was identified in the 5′-untranslated region (5′UTR) of the *IFITM5* gene and was later confirmed in other OI type V patient cohorts [5,10,12,13,17,18]. The mutation results in the addition of 5 amino acid residues (MALEP) at the N terminus of BRIL and to an apparent gain of function [13]. It has to be noted that a non-classical *IFITM5* mutation (c.119C> T; p.S40L) has been recently described as causing very severe OI phenotype with prenatal onset and showing an OI type VI rather than OI type V bone phenotype [19–21]. This novel mutation was not in the scope of the present work.

The bone fragility in human OI and in mouse models of the disease is at least in part caused by low bone volume and alterations in bone material [22–25]. Indeed, OI bone is more brittle due to higher mineral content, altered collagen properties and impaired bone

nanostructure [23,25–29]. We and other reported that mineral content on the material level is abnormally high in "classical" OI (types I, III and IV), independent of whether the underlying mutation affects collagen structure or causes haploinsufficiency. [26,30,31]. Furthermore, elevated matrix mineralization was found also in patients with a loss-of-function of PEDF (OI type VI), CRTAP (OI type VII), prolyl 3-hydroxylase 1 (OI type VIII) [32] or mutations in procollagen C-propeptide cleavage site or *BMP1* [33–36].

While clinical and radiological abnormalities in OI type V are well characterized, it is not yet clear whether the mutation affects bone matrix mineralization. At the cellular level, primary osteoblast cultures from OI type V patients show increased mineralization concomitantly with increased osteoblast differentiation markers but decreased type I collagen expression and altered fibrils appearance [13]. Jones et al, investigated five bone biopsy samples by backscattered electron imaging and noted increased mineralization of the bone matrix [37]. Apart this descriptive study, the mineralization of the "mesh-like" bone matrix in these patients has not been explored.

In the present study we used transiliac bone biopsy samples obtained from 15 individuals with OI type V and performed bone mineralization density distribution (BMDD) measurements by quantitative Backscattered Electron Imaging (qBEI). In a subset of patients treated with a bisphosphonate, we evaluated the mineral content of the bone matrix before and after pamidronate therapy (paired biopsy samples). Furthermore, we took advantage of the backscattered electron imaging method to quantify also the osteocyte lacunar density and size in cancellous and cortical bone.

MATERIAL AND METHODS

Patient cohort

The study cohort consisted of 15 treatment-naïve patients (male n=8, female n=7) with OI type V who are followed either at the Shriners Hospital for Children in Montreal, Canada (n=12) or at NIH, Bethesda, MD, USA (n=3) and who underwent a transiliac biopsy. The age of the patients at biopsy ranged from 1.8 to 14.8 years (8.7±4 y). None of the children have received pharmacological treatment prior the first iliac crest bone biopsy. All the patients had characteristic radiological, clinical and histology findings as already described [4,6,13] and were all carriers of the heterozygous *IFITM5* c.-14C>T mutation. None of our patients had the non-classical *IFITM5* mutation (c.119C> T; p.S40L).

Additionally, 8 of these patients were treated with cyclic intravenous pamidronate and underwent a post-treatment biopsy.

Informed consent from the subject and/or a legal guardian was obtained in each case. The study protocol was approved by the Ethics Committee of the Shriners Hospital and NICHD/NIH IRB.

Sample preparation

We used residual polymethylmethacrylate embedded sample blocks prepared for bone histomorphometry and reported previously [4,6]. Blocks were trimmed using a low speed

diamond saw (Isomet-R, Buehler Ltd. Lake Buff, IL, USA). Sectioned bone surfaces were sequentially ground with sand paper with increasing grid number followed by polishing with diamond grains (size down to 1 microns) on hard polishing clothes by a PM5 Logitech instrument (Glasgow, Scotland). Finally the sample surface was carbon coated by vacuum evaporation (Agar SEM Carbon Coater, Stansted, UK).

Quantitative Backscattered Electron Imaging (qBEI)

The details and validation of the qBEI method have been published elsewhere [38]. Briefly, qBEI is based on the fact that the intensity of electrons backscattered from the surface-layer of a sectioned bone area is proportional to the concentration of mineral (hydroxyapatite) and thus calcium in bone. A digital scanning electron microscope (DSM 962, Zeiss, Oberkochen, Germany) was employed with an accelerating voltage of 20 kV, a working distance of 15 mm and a probe current of 110 ± 4 pA. Backscattered electrons (BE) were measured by a four-quadrant semiconductor backscattered electron detector. Tissue areas were recorded with a pixel depth of 256 gray levels using a scan speed of 100 seconds per frame. For Bone Mineral Density Distribution (BMDD) analyses, a 50x nominal magnification (corresponding to a spatial resolution of 3.5 μm per pixel) was used whereas for osteocyte lacunar analyses, the scans were made with 200x magnification (corresponding to a spatial resolution of 0.9 μm per pixel).

Bone Mineral Density Distribution (BMDD)

From the digital images obtained by qBEI, gray level histograms were converted into calcium concentration values (weight % Ca) as reported previously [38,39]. In this method, one grey level step represents 0.17 weight % Ca. Such calcium content frequency histograms are called Bone Mineral Density Distribution.

BMDD was determined separately in cancellous bone and as the arithmetical mean of the 2 cortices in cortical bone of the transiliac biopsy samples. For comparison the BMDD is described by 5 parameters: the mean calcium concentration (CaMean; weighted mean calcium content), the most frequently occurring calcium concentration (CaPeak; the peak position of the BMDD) in the sample, the width of the BMDD distribution (CaWidth; full width at half maximum) reflecting the heterogeneity in matrix mineralization; the percentage of lowly mineralized bone, CaLow, is defined as the area below 17.68 weight% calcium. This cut-off corresponds to the 5^{th} percentile of the reference BMDD in human adults [40]. In a similar manner, the percentage of highly mineralized bone, CaHigh, is defined as the area above the 95^{th} percentile of the reference BMDD in human adults (25.30 weight% calcium).

Osteocyte lacunae section analyses

To characterize the osteocyte lacunae, 2D image analyses were performed. Basically, an Osteocyte Lacunae (OL) is defined as a 3D cavity within the mineralized bone matrix occupied by an osteocyte. After sample preparation, bone surfaces with Osteocyte Lacuna Sections (OLS) *i.e.* 2D sectioned area of OL are obtained.

qBEI images with pixel resolution of 0.88 μm/pixel were used to perform the 2D analyses of osteocyte lacunae sections using a custom-made macro in ImageJ software (1.50f)[41]. We

set a minimal bone area of 0.5 mm^2 to be appropriate for OLS analyses. A grey level threshold to discriminate between mineralized bone matrix and OLS area was set at a fixed grey level of 55 (Ca wt % 5.2). A size threshold to discriminate OLS from either surrounding mineralized bone matrix or from the osteonal channels was set between 5μm^2 and 80 μm^2.

Five parameters were characterized: (1) OLS-density, the number of OLS per mineralized bone matrix area; (2) OLS-porosity, OLS total area / (mineralized bone matrix area+ OLS total area); (3) OLS-area, mean value of the OLS areas per sample; (4) OLS-perimeter, mean value of the OLS perimeters per sample; (5) OLS-AR, mean value of the OLS aspect ratio (AR) per sample. AR is a measure of elongation to describe the particle's fitted ellipse: (Major Axis)/(Minor Axis). A value of 1 indicates a perfect circle and increasing values indicate increasingly elongated shape. Values > 10 were excluded.

References

The qBEI results were compared with data obtained in a young reference cohort (age range from 1.5 to 23 years) described elsewhere [42].

For osteocyte lacunae comparison, we analyzed transiliac biopsies of 6 healthy control children of similar age (range from 2 to 9.4 years; mean 6.6±3.5y) who are a subcohort from a previous study [42]. All samples were intact consisting of 2 cortices and trabecular bone.

Statistical analyses

The data are presented as median with interquartile range [25th; 75th percentiles]. Statistical analyses were carried out with the Graphpad Prism 6.01 program (GraphPad Software, Inc., La Jolla, CA, USA). Non-parametrical tests were used due to the low sample number or the non-Gaussian distribution of the values. qBEI and OL data from the patients were compared to the reference group using Mann-Whitney test. Data before and after treatment were compared by Wilcoxon matched-pair rank test. Differences were considered statistically significant at $p<0.05$.

RESULTS

BMDD in OI type V

Figure 1 shows typical BMDD curves (solid lines) from cancellous and cortical regions of a transiliac biopsy sample obtained from a 4-year-old child with OI type V. BMDD from both regions was clearly shifted towards higher matrix mineralization compared to the young reference cohort [42]. Consistently in our study cohort, the BMDD parameters CaMean, CaPeak, CaHigh were significantly increased in both cancellous and cortical bone, as shown in Figure 2 and Table 1.

BMDD changes after bisphosphonate treatment

Figure 1 also shows an example of BMDD curves from cancellous and cortical bone obtained after 2.6 years bisphosphonate treatment (dotted lines). It can be seen that the curves were only slightly shifted towards higher mineralization compared to pre-treatment.

A pairwise comparison before and after treatment (n=8) (Figure 3) revealed an increase of CaMean in cancellous (+3%, P<0.05) and cortical (+2.8%, P<0.05) regions but CaPeak was not significantly changed. Moreover CaHigh (+60%, P<0.05) appeared significantly higher only in cancellous bone, whereas CaLow was lower in cancellous (−25%, P<0.05) and cortical (−31%, P<0.05) bone. The heterogeneity of bone matrix mineralization (CaWidth) was similar before and after treatment.

Characteristics of osteocyte lacunae

Figure 4 shows typical backscattered images of cortical and trabecular bone in transiliac biopsy samples from control (A and B, respectively) and OI type V (C and D, respectively). A higher number of OLS is obvious in both cortical and cancellous bone from OI type V compared to the control sample.

Consistently the OLS analyses in cortical bone (Table 1) from all OI type V samples (n=15) revealed an increase of OLS-porosity (+295%, P<0.0001), of OLS-density (+171%, P<0.0001), of the size parameters OLS-area (+26 %, P<0.001) and OLS-perimeter (+23%, P<0.0001), and of the shape parameter OLS-AR (+22%, P<0.01) compared to reference samples (n=6).

The findings in cancellous bone (n=5) (Table 1) were similar, with an increase of OLS-porosity (+215%, P<0.01), OLS-density (+183%, P<0.01) and OLS-perimeter (+7 %, P<0.01) compared to the reference. The increase of OLS-area (+5%) and OLS-AR (+6%) did not reach significance.

In the cortices of some control samples we observed regions with primary periosteal bone formation. As previously reported [42], these areas appeared to be more highly mineralized and to contain more osteocyte lacunae than the adjacent osteonal bone (see arrows in Figure 4A). These similarities to the OI type V samples prompted us to perform polarized light microscopy images from cortical bone sections of the transiliac biopsy samples. We observed disorganized collagen fibril orientation in type V OI bone throughout the whole bone area (cortex and cancellous bone). This pattern appeared very similar to the region with primary periosteal bone apposition in control samples (Fig. 5).

DISCUSSION

The present study demonstrates that bone matrix mineralization is shifted towards higher values in children with OI type V compared to a young healthy reference cohort, comparable to the hypermineralization found in bone with classical OI. Treatment with bisphosphonate results in a further slight elevation of the mineralization. The 2D analysis of sectioned osteocyte lacunar areas shows an increase in number and size of osteocyte lacunae compared to healthy control bone.

The qBEI analyses revealed hypermineralization of bone matrix in OI type V compared to healthy children, as reflected by the significant increase of CaMean, CaPeak and, most remarkably, CaHigh in both cancellous and cortical bone. Hypermineralization seems to be a characteristic feature of OI in humans as well as in mouse models [26,30,31,33,34,43].

Structural changes in the procollagen chains are probably not the direct cause of this hypermineralization, since it is also observed in OI caused by *COL1A1* haploinsufficiency mutations [30] and in mutations affecting genes whose products interact post-translationally with type I collagen and alter its modification, as in types VII and VIII OI (folding, processing, modification, chaperoning…) [33–35].

Interestingly, bisphosphonate treatment increased bone mineral content only marginally. In high bone turnover osteoporosis, antiresorptive treatments leads to higher mineral content, which is explained by the fact that lower bone turnover allows for more time to mineralize [44]. In "classical" OI or in OI mouse models, bisphosphonates do not seem to have an additional effect on bone mineralization [31,43]. In OI type V, while CaPeak remained unchanged, higher CaMean was associated with lower CaLow, which is in line with the strongly reduced bone remodeling, as already reported [6]. The modest increase of CaMean is most likely due to the already high mineral content. Hence, the treatment effect is the increase in bone mineral density measured by dual-energy X-ray absorptiometry mainly linked to the elevation of bone volume and mineralized cartilage, as previously observed in these OI type V patients [6] and in other OI types [22,45].

At first glance the hypermineralization of bone in OI type V is somewhat surprising, considering that BRIL has no direct collagen-related function. However the gain-of-function BRIL mutation leads to a decrease of osteoblast collagen production [13]. Moreover our results are consistent with the *in vitro* findings of dose-dependent effect of Ifitm5 levels on mineralization in a rat osteosarcoma cell line [16] and increase of mineralization in human osteoblasts in culture [13].

The most characteristic features of OI type V bone at the tissue level are the "mesh-like" appearance of the bone matrix and the lack of regular bone lamellation (Figure 5C) [4], the tremendous increase of osteocyte lacunar density and size, as well as bone matrix hypermineralization. Collectively, this could indicate an osteoblast dysfunction consistent with the faulty intracellular activity of mutant MALEP-BRIL [46]. It still remains unclear how the heterozygous BRIL mutation results in the OI type V phenotype. It has to be noted that such bone characteristics were also partly described in other forms of OI [37,45,47,48]. Remarkably, we observe that the hypermineralization associated with high osteocyte lacunar number and disturbed lamellation are also characteristic for the primary bone formed in the periosteal bone apposition during normal skeletal development [42,49]. Therefore the striking similarities of OI type V bone to primary bone lead us to hypothesize that BRIL might be essential in primary bone formation by osteoblasts. This would be in line with BRIL expression in early steps of bone formation in calvaria and the bone collar surrounding the developing long-bones in mice and rats [16]. Consequently, the gain-of-function mutation might lead to an overproduction of periosteal primary bone and / or to impaired formation of ordered lamellar bone in the phase of secondary bone formation during bone remodeling. Indeed, haversian canals and bone packets delineated by cement lines were also viewed in OI type V bone consistent with resorption indices within normal range as revealed by bone histomorphometry. However, scanning electron and light microscopy did not reveal noticeable differences in the bone matrix structure between periosteal primary and osteonal /

secondary bone in OI type V (Figure 4C). This would suggest that the remarkable mesh-like collagen lamellation is a kind of primary bone, even if formed during bone remodeling.

Our hypothesis is also consistent with the overall clinical picture of OI type V which suggests enhanced primary bone formation processes. Exuberant callus formation, a hallmark for OI type V, develops often after fractures and sometime without any fracture history [7]. This hyperplastic callus is histologically heterogeneous and contains hypercellular woven bone [50,51]. The so-called 'calcification of the forearm interosseous membrane', another type V OI hallmark, has been described not as an ectopic calcification but rather caused by dysregulated periosteal proliferation [5]. Consistently, the heterotopic ossifications in the muscles and tendons attached to the pelvic bone and femur described by Kim et al. [52] also strengthens the hypothesis of a profound disturbance in the process of bone formation.

The main limitation of our study is the relative low sample number due to the rarity of OI type V. Moreover, the scarcity of cancellous bone in some biopsy samples restricted the number specimen available for trabecular BMDD measurements and osteocyte lacunar analysis. Nevertheless we observed highly significant differences in degree of mineralization and in characteristics of osteocyte lacunae between the patients and the reference values.

In summary, the bone material from OI type V patients is highly mineralized. On the one hand, this finding is similar to the other forms of OI, although type V OI does not alter collagen structure or modification. In addition, the lack of regular bone lamellation associated with elevated osteocyte lacunar density supports the idea of an exuberant primary bone formation, associated with an alteration of the bone remodeling process as underlying the unique features of type V OI bone formation.

Acknowledgments

This study was supported by the Shriners of North America, the AUVA (Research funds of the Austrian workers compensation board) and the WGKK (Viennese sickness insurance funds) as well as NICHD/NIH, USA intramural funding (JCM). We thank Sonja Lueger, Daniela Gabriel, Petra Keplinger and Phaedra Messmer for excellent technical assistance at the bone material laboratory of the Ludwig Boltzmann Institute of Osteology, Vienna, Austria.

Authors' roles: Study design: SB, NFZ, PR, JCM and FR. Study conduct and data collection: SB, NFZ, PR, JCM and FR. Data analysis: SB, NFZ, PR. Data interpretation: SB, NFZ, FHG, PR, KK, JCM and FR. Drafting manuscript: SB, NFZ, PR. All authors revised the manuscript content and approved the final version of the manuscript. SB takes responsibility for the integrity of the data analysis.

References

1. Forlino A, Cabral WA, Barnes AM, Marini JC. New perspectives on osteogenesis imperfecta. Nature reviews Endocrinology. Sep; 2011 7(9):540–57.
2. Sillence DO, Senn A, Danks DM. Genetic heterogeneity in osteogenesis imperfecta. Journal of medical genetics. Apr; 1979 16(2):101–16. [PubMed: 458828]
3. Forlino A, Marini JC. Osteogenesis imperfecta. Lancet. Apr 16; 2016 387(10028):1657–71. [PubMed: 26542481]
4. Glorieux FH, Rauch F, Plotkin H, Ward L, Travers R, Roughley P, et al. Type V osteogenesis imperfecta: a new form of brittle bone disease. Journal of bone and mineral research : the official journal of the American Society for Bone and Mineral Research. Sep; 2000 15(9):1650–8.

5. Rauch F, Moffatt P, Cheung M, Roughley P, Lalic L, Lund AM, et al. Osteogenesis imperfecta type V: marked phenotypic variability despite the presence of the IFITM5 c.14C>T mutation in all patients. Journal of medical genetics. Jan; 2013 50(1):21–4. [PubMed: 23240094]
6. Zeitlin L, Rauch F, Travers R, Munns C, Glorieux FH. The effect of cyclical intravenous pamidronate in children and adolescents with osteogenesis imperfecta type V. Bone. Jan; 2006 38(1):13–20. [PubMed: 16162424]
7. Cheung MS, Glorieux FH, Rauch F. Natural history of hyperplastic callus formation in osteogenesis imperfecta type V. Journal of bone and mineral research : the official journal of the American Society for Bone and Mineral Research. Aug; 2007 22(8):1181–6.
8. Grover M, Campeau PM, Lietman CD, Lu JT, Gibbs RA, Schlesinger AE, et al. Osteogenesis imperfecta without features of type V caused by a mutation in the IFITM5 gene. Journal of bone and mineral research : the official journal of the American Society for Bone and Mineral Research. Nov; 2013 28(11):2333–7.
9. Semler O, Garbes L, Keupp K, Swan D, Zimmermann K, Becker J, et al. A mutation in the 5′-UTR of IFITM5 creates an in-frame start codon and causes autosomal-dominant osteogenesis imperfecta type V with hyperplastic callus. American journal of human genetics. Aug 10; 2012 91(2):349–57. [PubMed: 22863195]
10. Shapiro JR, Lietman C, Grover M, Lu JT, Nagamani SC, Dawson BC, et al. Phenotypic variability of osteogenesis imperfecta type V caused by an IFITM5 mutation. Journal of bone and mineral research : the official journal of the American Society for Bone and Mineral Research. Jul; 2013 28(7):1523–30.
11. Cho TJ, Lee KE, Lee SK, Song SJ, Kim KJ, Jeon D, et al. A single recurrent mutation in the 5′-UTR of IFITM5 causes osteogenesis imperfecta type V. American journal of human genetics. Aug 10; 2012 91(2):343–8. [PubMed: 22863190]
12. Lazarus S, McInerney-Leo AM, McKenzie FA, Baynam G, Broley S, Cavan BV, et al. The IFITM5 mutation c.14C > T results in an elongated transcript expressed in human bone; and causes varying phenotypic severity of osteogenesis imperfecta type V. BMC musculoskeletal disorders. 2014; 15:107. [PubMed: 24674092]
13. Reich A, Bae AS, Barnes AM, Cabral WA, Hinek A, Stimec J, et al. Type V OI primary osteoblasts display increased mineralization despite decreased COL1A1 expression. The Journal of clinical endocrinology and metabolism. Feb; 2015 100(2):E325–32. [PubMed: 25387264]
14. Rauch F, Lalic L, Roughley P, Glorieux FH. Relationship between genotype and skeletal phenotype in children and adolescents with osteogenesis imperfecta. Journal of bone and mineral research : the official journal of the American Society for Bone and Mineral Research. Jun; 2010 25(6): 1367–74. Epub 2009/11/26.
15. Hanagata N, Li X, Morita H, Takemura T, Li J, Minowa T. Characterization of the osteoblast-specific transmembrane protein IFITM5 and analysis of IFITM5-deficient mice. Journal of bone and mineral metabolism. May; 2011 29(3):279–90. [PubMed: 20838829]
16. Moffatt P, Gaumond MH, Salois P, Sellin K, Bessette MC, Godin E, et al. Bril: a novel bone-specific modulator of mineralization. Journal of bone and mineral research : the official journal of the American Society for Bone and Mineral Research. Sep; 2008 23(9):1497–508.
17. Brizola E, Mattos EP, Ferrari J, Freire PO, Germer R, Llerena JC Jr, et al. Clinical and Molecular Characterization of Osteogenesis Imperfecta Type V. Molecular syndromology. Oct; 2015 6(4): 164–72. [PubMed: 26648832]
18. Balasubramanian M, Parker MJ, Dalton A, Giunta C, Lindert U, Peres LC, et al. Genotype-phenotype study in type V osteogenesis imperfecta. Clinical dysmorphology. Jul; 2013 22(3):93–101. [PubMed: 23612438]
19. Farber CR, Reich A, Barnes AM, Becerra P, Rauch F, Cabral WA, et al. A novel IFITM5 mutation in severe atypical osteogenesis imperfecta type VI impairs osteoblast production of pigment epithelium-derived factor. Journal of bone and mineral research : the official journal of the American Society for Bone and Mineral Research. Jun; 2014 29(6):1402–11.
20. Guillen-Navarro E, Ballesta-Martinez MJ, Valencia M, Bueno AM, Martinez-Glez V, Lopez-Gonzalez V, et al. Two mutations in IFITM5 causing distinct forms of osteogenesis imperfecta. American journal of medical genetics Part A. May; 2014 164A(5):1136–42. [PubMed: 24478195]

21. Hoyer-Kuhn H, Semler O, Garbes L, Zimmermann K, Becker J, Wollnik B, et al. A nonclassical IFITM5 mutation located in the coding region causes severe osteogenesis imperfecta with prenatal onset. Journal of bone and mineral research : the official journal of the American Society for Bone and Mineral Research. Jun; 2014 29(6):1387–91.
22. Fratzl-Zelman N, Misof BM, Klaushofer K, Roschger P. Bone mass and mineralization in osteogenesis imperfecta. Wiener medizinische Wochenschrift. Jul; 2015 165(13–14):271–7. [PubMed: 26208477]
23. Vanleene M, Porter A, Guillot PV, Boyde A, Oyen M, Shefelbine S. Ultra-structural defects cause low bone matrix stiffness despite high mineralization in osteogenesis imperfecta mice. Bone. Jun; 2012 50(6):1317–23. Epub 2012/03/28. [PubMed: 22449447]
24. Paschalis EP, Gamsjaeger S, Fratzl-Zelman N, Roschger P, Masic A, Brozek W, et al. Evidence for a Role for Nanoporosity and Pyridinoline Content in Human Mild Osteogenesis Imperfecta. Journal of bone and mineral research : the official journal of the American Society for Bone and Mineral Research. May; 2016 31(5):1050–9.
25. Bishop N. Bone Material Properties in Osteogenesis Imperfecta. Journal of bone and mineral research : the official journal of the American Society for Bone and Mineral Research. Apr; 2016 31(4):699–708.
26. Boyde A, Travers R, Glorieux FH, Jones SJ. The mineralization density of iliac crest bone from children with osteogenesis imperfecta. Calcified tissue international. Mar; 1999 64(3):185–90. [PubMed: 10024373]
27. Camacho NP, Hou L, Toledano TR, Ilg WA, Brayton CF, Raggio CL, et al. The material basis for reduced mechanical properties in oim mice bones. Journal of bone and mineral research : the official journal of the American Society for Bone and Mineral Research. Feb; 1999 14(2):264–72.
28. Fratzl P, Paris O, Klaushofer K, Landis WJ. Bone mineralization in an osteogenesis imperfecta mouse model studied by small-angle x-ray scattering. The Journal of clinical investigation. Jan 15; 1996 97(2):396–402. [PubMed: 8567960]
29. Fratzl-Zelman N, Schmidt I, Roschger P, Glorieux FH, Klaushofer K, Fratzl P, et al. Mineral particle size in children with osteogenesis imperfecta type I is not increased independently of specific collagen mutations. Bone. Mar.2014 60:122–8. [PubMed: 24296239]
30. Roschger P, Fratzl-Zelman N, Misof BM, Glorieux FH, Klaushofer K, Rauch F. Evidence that abnormal high bone mineralization in growing children with osteogenesis imperfecta is not associated with specific collagen mutations. Calcified tissue international. Apr; 2008 82(4):263–70. [PubMed: 18311573]
31. Weber M, Roschger P, Fratzl-Zelman N, Schoberl T, Rauch F, Glorieux FH, et al. Pamidronate does not adversely affect bone intrinsic material properties in children with osteogenesis imperfecta. Bone. Sep; 2006 39(3):616–22. [PubMed: 16644299]
32. Fratzl-Zelman N, Barnes AM, Weis M, Carter E, Hefferan TE, Perino G, et al. Non-Lethal Type VIII Osteogenesis Imperfecta Has Elevated Bone Matrix Mineralization. The Journal of clinical endocrinology and metabolism. Sep; 2016 101(9):3516–25. [PubMed: 27383115]
33. Fratzl-Zelman N, Morello R, Lee B, Rauch F, Glorieux FH, Misof BM, et al. CRTAP deficiency leads to abnormally high bone matrix mineralization in a murine model and in children with osteogenesis imperfecta type VII. Bone. Mar; 2010 46(3):820–6. [PubMed: 19895918]
34. Fratzl-Zelman N, Schmidt I, Roschger P, Roschger A, Glorieux FH, Klaushofer K, et al. Unique micro- and nano-scale mineralization pattern of human osteogenesis imperfecta type VI bone. Bone. Apr.2015 73:233–41. [PubMed: 25554599]
35. Lindahl K, Barnes AM, Fratzl-Zelman N, Whyte MP, Hefferan TE, Makareeva E, et al. COL1 C-propeptide cleavage site mutations cause high bone mass osteogenesis imperfecta. Human mutation. Jun; 2011 32(6):598–609. [PubMed: 21344539]
36. Hoyer-Kuhn H, Semler O, Schoenau E, Roschger P, Klaushofer K, Rauch F. Hyperosteoidosis and hypermineralization in the same bone: bone tissue analyses in a boy with a homozygous BMP1 mutation. Calcified tissue international. Dec; 2013 93(6):565–70. [PubMed: 24091809]
37. Jones SJ, Glorieux FH, Travers R, Boyde A. The microscopic structure of bone in normal children and patients with osteogenesis imperfecta: a survey using backscattered electron imaging. Calcified tissue international. Jan; 1999 64(1):8–17. [PubMed: 9868277]

38. Roschger P, Fratzl P, Eschberger J, Klaushofer K. Validation of quantitative backscattered electron imaging for the measurement of mineral density distribution in human bone biopsies. Bone. Oct; 1998 23(4):319–26. [PubMed: 9763143]
39. Roschger P, Plenk H Jr, Klaushofer K, Eschberger J. A new scanning electron microscopy approach to the quantification of bone mineral distribution: backscattered electron image grey-levels correlated to calcium K alpha-line intensities. Scanning microscopy. Mar; 1995 9(1):75–86. discussion –8. [PubMed: 8553027]
40. Roschger P, Gupta HS, Berzlanovich A, Ittner G, Dempster DW, Fratzl P, et al. Constant mineralization density distribution in cancellous human bone. Bone. Mar; 2003 32(3):316–23. [PubMed: 12667560]
41. Schneider CA, Rasband WS, Eliceiri KW. NIH Image to ImageJ: 25 years of image analysis. Nature methods. Jul; 2012 9(7):671–5. [PubMed: 22930834]
42. Fratzl-Zelman N, Roschger P, Misof BM, Pfeffer S, Glorieux FH, Klaushofer K, et al. Normative data on mineralization density distribution in iliac bone biopsies of children, adolescents and young adults. Bone. Jun; 2009 44(6):1043–8. [PubMed: 19268565]
43. Misof BM, Roschger P, Baldini T, Raggio CL, Zraick V, Root L, et al. Differential effects of alendronate treatment on bone from growing osteogenesis imperfecta and wild-type mouse. Bone. Jan; 2005 36(1):150–8. [PubMed: 15664013]
44. Roschger P, Paschalis EP, Fratzl P, Klaushofer K. Bone mineralization density distribution in health and disease. Bone. Mar; 2008 42(3):456–66. [PubMed: 18096457]
45. Rauch F, Glorieux FH. Osteogenesis imperfecta. Lancet. Apr 24; 2004 363(9418):1377–85. [PubMed: 15110498]
46. Patoine A, Gaumond MH, Jaiswal PK, Fassier F, Rauch F, Moffatt P. Topological mapping of BRIL reveals a type II orientation and effects of osteogenesis imperfecta mutations on its cellular destination. Journal of bone and mineral research : the official journal of the American Society for Bone and Mineral Research. Sep; 2014 29(9):2004–16.
47. Imbert L, Auregan JC, Pernelle K, Hoc T. Microstructure and compressive mechanical properties of cortical bone in children with osteogenesis imperfecta treated with bisphosphonates compared with healthy children. Journal of the mechanical behavior of biomedical materials. Jun.2015 46:261–70. [PubMed: 25828157]
48. Rauch F, Travers R, Parfitt AM, Glorieux FH. Static and dynamic bone histomorphometry in children with osteogenesis imperfecta. Bone. Jun; 2000 26(6):581–9. [PubMed: 10831929]
49. Currey JD. The many adaptations of bone. Journal of biomechanics. Oct; 2003 36(10):1487–95. [PubMed: 14499297]
50. Brenner RE, Vetter U, Nerlich A, Worsdorfer O, Teller WM, Muller PK. Biochemical analysis of callus tissue in osteogenesis imperfecta type IV. Evidence for transient overmodification in collagen types I and III. The Journal of clinical investigation. Sep; 1989 84(3):915–21. [PubMed: 2760218]
51. Fairbank HA. Hyperplastic callus formation, with or without evidence of a fracture, in osteogenesis imperfecta. The British journal of surgery. Jul; 1948 36(141):1–16. [PubMed: 18880323]
52. Kim OH, Jin DK, Kosaki K, Kim JW, Cho SY, Yoo WJ, et al. Osteogenesis imperfecta type V: clinical and radiographic manifestations in mutation confirmed patients. American journal of medical genetics Part A. Aug; 2013 161A(8):1972–9. [PubMed: 23804581]

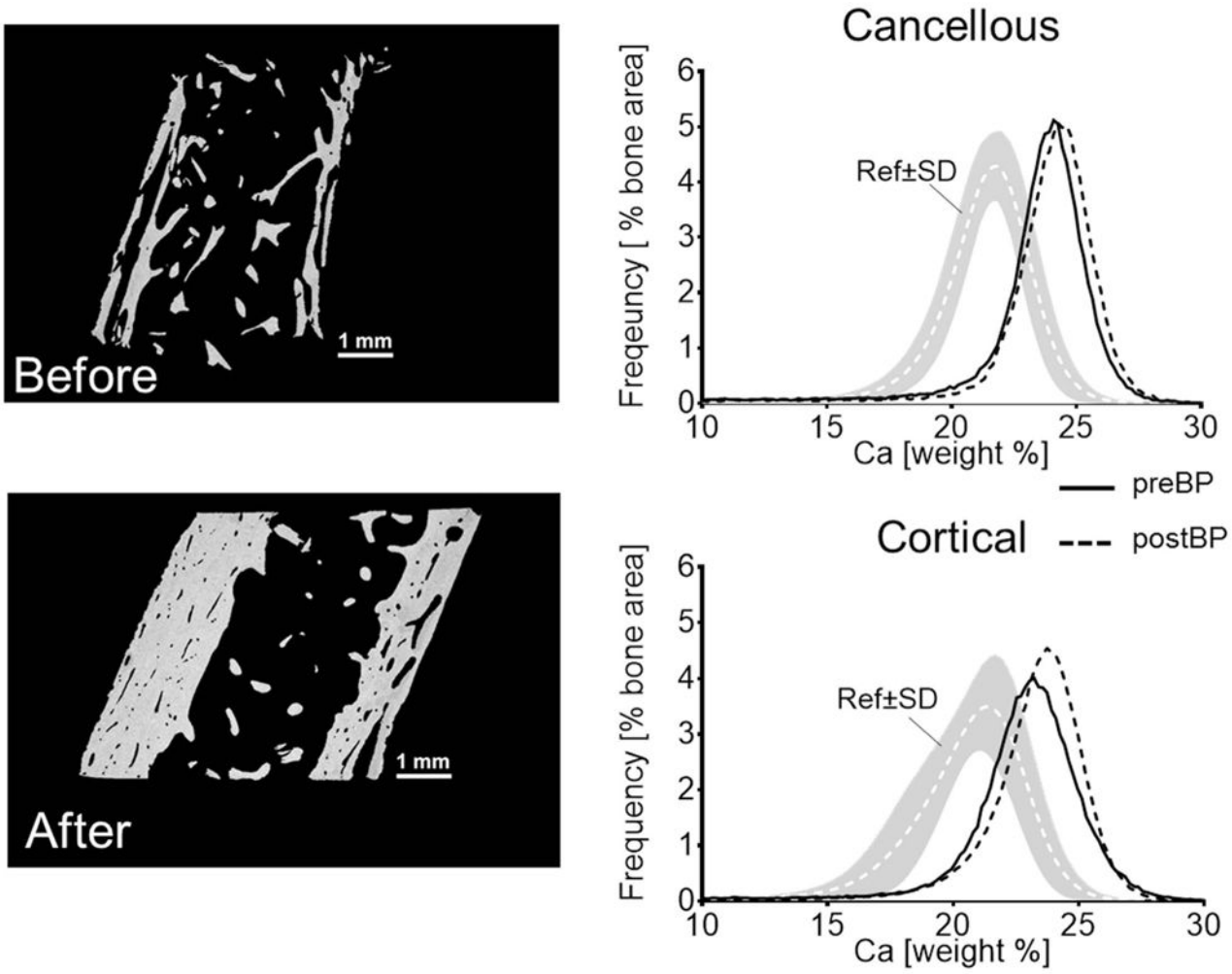

Figure 1.

Example of cancellous and cortical BMDD measurements of transiliac bone biopsy samples (overview images by backscatter electron imaging) from a 4 years old girl with OI type V before bisphosphonate treatment (preBP - solid line) and after 2.6 years (postBP - dotted line); Ref= reference data base of healthy children [(42)].

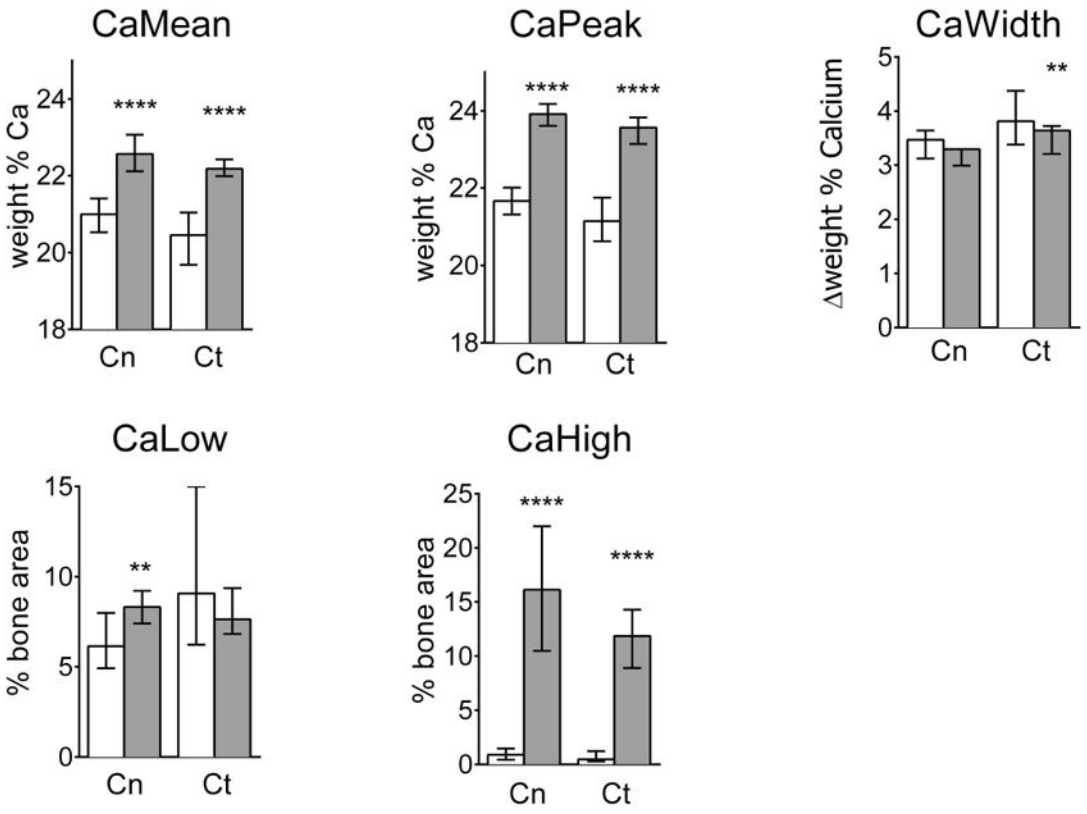

Figure 2.

Statistical comparison of BMDD parameter values between reference data base (white bars) of healthy children bone and OI-V bone (grey bars) for the cancellous (Cn) and cortical (Ct) bone compartments before treatment. Mann Whitney test: **p<0.01, ***p<0.0001; bars: median; error bars: interquartile range; Sample size: Cn: n=12; Ct : n=15

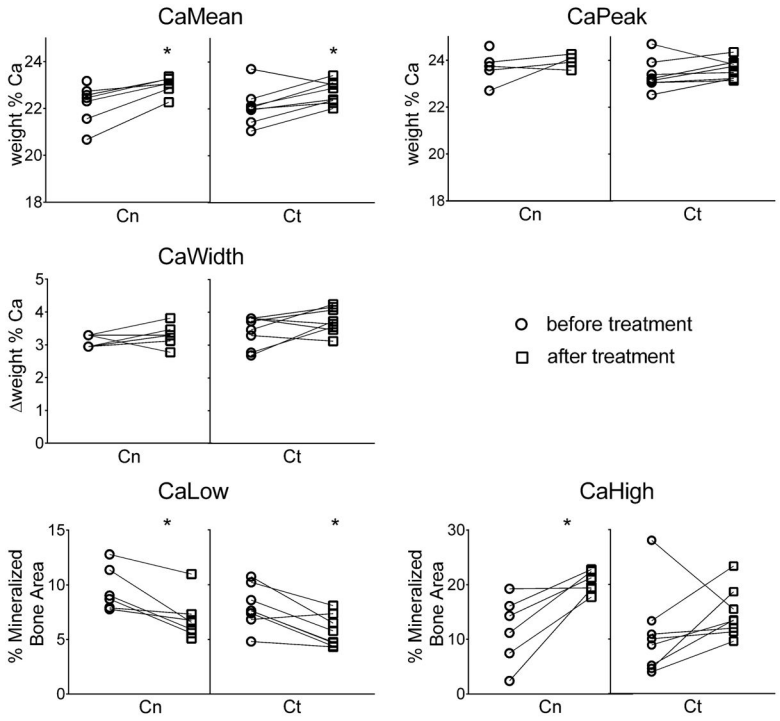

Figure 3.

Paired comparison of BMDD parameter values obtained before and after bisphosphonate treatment in OI type V patients for cancellous (Cn) and cortical bone (Ct); *p<0.05; sample size: Cn: n=6, Ct: n=8

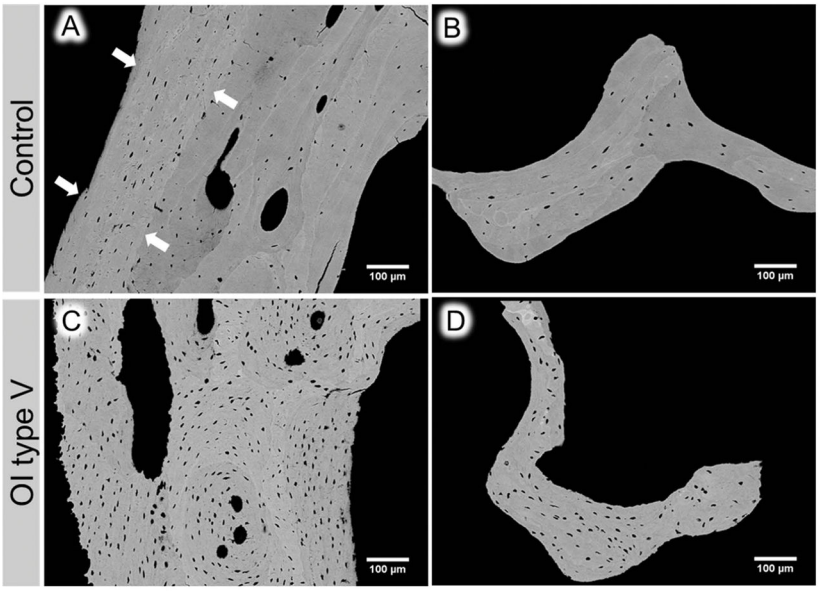

Figure 4.

qBEI images of cortical (A, C) and trabecular (B, D) bone area obtained on biopsy samples from control (A &B) and OI type V (C & D) affected children. Note the increased osteocyte lacunar density in the area of periosteal primary bone (delimitated by white arrows) in the cortical compartment of the control biopsy (white arrows in A). Osteocyte lacunar density seems lower within the adjacent secondary, remodeled bone and in the trabeculae. In contrast, in OI type V bone a high density of osteocyte lacunae can be observed in both cortical and trabecular area.

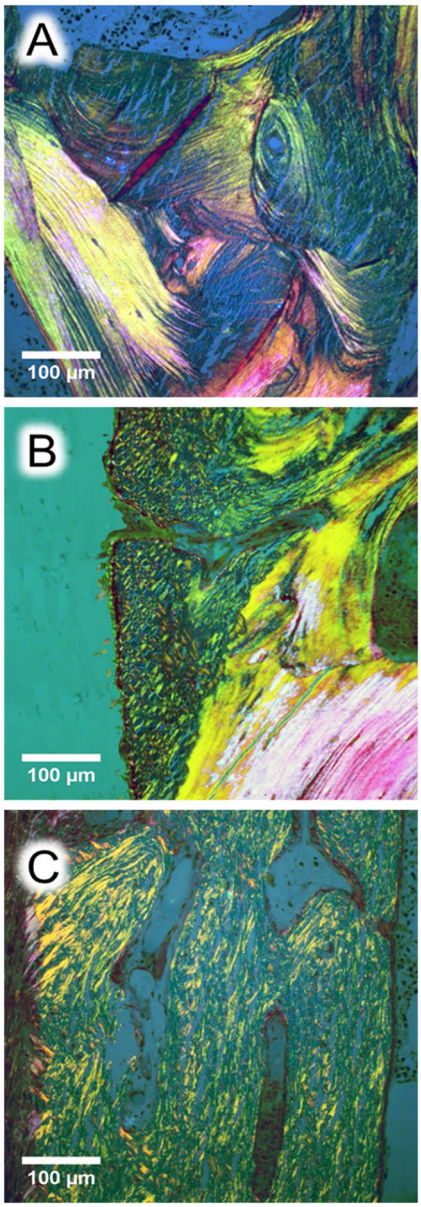

Figure 5.

Histological images of cortical bone from transiliac biopsy samples (A and B: control, C: OI type V). The sections were stained by Goldner trichrome and observed in polarized light. (A) Ordered lamellar collagen organization in a healthy control (2 year-old child), (B) periosteal primary bone apposition in the same child viewed as disorganized collagen fibrils pattern abutting to the secondary remodeled bone with lamellar pattern, (C) collagen organization in a 6.8 year-old child with OI type V suggesting short range and randomly organized fibril throughout the cortex similarly to the periosteal primary bone apposition observed in B.

Table 1

Results of backscattered images analyses in cancellous (Cn) and cortical (Ct) bone compartments from OI type V patients before treatment compared to reference data base

	Cn		Ct	
	OI type V[a]	**Reference[b]**	**OI type V[a]**	**Reference[b]**
BMDD variables				
CaMean [wt% Ca]	22.57 **** [22.11;23.06]	21.00 [20.53; 21.40]	22.18 **** [21.99; 22.42]	20.45 [19.68; 21.04]
CaPeak [wt% Ca]	23. 92 **** [23.61; 24.18]	21.66 [21.32; 22.01]	23.57 **** [23.14; 23.83]	21.14 [20.62; 21.75]
CaWidth [Δwt% Ca]	3.29 [2.99; 3.29]	3.47 [3.12; 3.64]	3.64 ** [3.21; 3.73]	3.81 [3.38; 4.38]
CaLow [% B.Ar]	8.31 ** [7.4; 9.22]	6.14 [4.92; 7.99]	7.63 [6.82; 9.37]	9.06 [6.22; 15.00]
CaHigh [% B.Ar]	16.13 **** [10.48; 22.01]	0.89 [0.43; 1.47]	11.85 **** [8.9; 14.28]	0.46 [0.28; 1.22]
OLS variables				
OLS-porosity [%]	1.48 ** [1.22; 1.75]	0.47 [0.43; 0.56]	2.29 **** [1.73; 2.44]	0.58 [0.56;0.66]
OLS-density [Nb OLS/mm^2]	646.4 ** [501; 800.8]	228.2 [200.7; 250]	816.5 **** [756.3; 922.5]	301.5 [262.9; 326.5]
OLS-area [µm^2]	22.9 [20.7; 26.8]	21.9 [20.3; 22.6]	25.4 *** [22.3; 27.7]	20.21 [18.71; 21.75]
OLS-perimeter [µm]	20.9 ** [20.4; 21.8]	19.5 [19.2; 19.9]	22.6 **** [21.3; 23.2]	18.4 [17.7; 19.6]
OLS-AR	2.83 [2.54; 3.12]	2.68 [2.44; 2.76]	2.92 ** [2.75; 3.29]	2.39 [2.31; 2.6]

Data shown are median with IQ range [25%; 75%]. OI type V vs Reference (Mann Whitney):

** p<0.01;

*** p<0.001;

**** p<0.0001.

[a] For qBEI measurement, 15 biopsy samples were evaluated (cortical n=15; cancellous n=12). For OLS analysis, the minimal bone area was achieved in 15 samples (cortical n=15; cancellous n=5).

[b] (38). The reference OLS data for Cn and Ct were obtained from 6 control children.